



ELSEVIER

Contents lists available at ScienceDirect

## Materials Letters

journal homepage: [www.elsevier.com/locate/matlet](http://www.elsevier.com/locate/matlet)

# Nanostructured porous cobalt oxide synthesis from $\text{Co}_3[\text{Co}(\text{CN})_6]_2$ and its possible applications in Lithium battery



Srinivasan Harish<sup>b</sup>, Krishnamoorthy Silambarasan<sup>a</sup>, Gopi Kalaiyaran<sup>a</sup>,  
Alam Venugopal Narendra Kumar<sup>a</sup>, James Joseph<sup>a,\*</sup>

<sup>a</sup> *Electronics and Electrocatalysis Division, CSIR – Central Electrochemical Research Institute, Karaikudi 630006, Tamil Nadu, India*

<sup>b</sup> *Department of Chemistry, PSG Institute of Technology and Applied Research, Neelambur, Coimbatore - 641062*

## ARTICLE INFO

## Article history:

Received 8 October 2015

Received in revised form

24 November 2015

Accepted 26 November 2015

Available online 27 November 2015

## Keywords:

Cobalt oxide

Nanoparticles

Energy storage and conversion

Porous material

Sensors

Thin films

## ABSTRACT

The thermal decomposition and microwave heating of  $\text{Co}_3[\text{Co}(\text{CN})_6]_2$  leads to formation of nanostructured porous cobalt oxide ( $\text{Co}_3\text{O}_4$ ). Here, we report  $\text{Co}_3[\text{Co}(\text{CN})_6]_2$  as a novel single source precursor for the synthesis of phase pure  $\text{Co}_3\text{O}_4$  particles at 650 °C under mixed argon/oxygen atmosphere as evidenced from X-ray diffraction (XRD) patterns. During thermal decomposition, release of gaseous products like  $\text{CO}_2$ ,  $\text{N}_x\text{O}_y$ ,  $(\text{CN})_2$  facilitate the formation of a highly porous  $\text{Co}_3\text{O}_4$  whose morphology and particle size distribution were characterized using scanning electron microscopy (SEM) and transmission electron microscopy (TEM) respectively. Porous  $\text{Co}_3\text{O}_4$  shows high discharge capacity of  $1131 \text{ mA h g}^{-1}$  with 96% coulombic efficiency against  $\text{Li}/\text{Li}^+$  reference electrode.

© 2015 Elsevier B.V. All rights reserved.

## 1. Introduction

Cobalt oxide ( $\text{Co}_3\text{O}_4$ ) attracts the attention of the materials researchers because of its promising applications in various fields viz., anode material for Li-ion batteries (LIBs) [1], super capacitors [2], gas sensors [3], catalytic processes [4] etc.  $\text{Co}_3\text{O}_4$  nanoparticles were synthesized through various routes that include the commonly employed oxidative precipitation [5], thermal decomposition [6,7], hydrothermal synthesis [8,9] etc., Synthesis of metal oxides like NiO,  $\text{Co}_3\text{O}_4$ , from single source precursors is a simple approach to make a porous structure for increasing material performance [10,11]. A few examples of single source precursors include  $(\text{NH}_4)_2\text{Co}_8(\text{CO}_3)_6(\text{OH})_6 \cdot 4\text{H}_2\text{O}$  [12],  $\text{Co}(\text{CO}_3)_{0.5}(\text{OH})_{0.1} \cdot 1\text{H}_2\text{O}$  [7,13],  $\text{Co}_4(\text{CO})_{12}$  [14], prussian blue [15]. Eppel's group have shown that how crystal structure of the precursor dictates the structure and morphology of the resulting products when thermolysis was carried out under moderate temperatures [16,17]. The catalytic activity towards the formation of methanol from synthetic gas ( $\text{CO}/\text{CO}_2/\text{H}_2$ ) was studied using Cu/ZnO catalyst. Surprisingly, catalytic activity was not observed on Cu/ZnO catalysts synthesized from  $\text{Cu}[\text{Zn}(\text{CN})_3]$  whereas the Cu/ZnO synthesized

from complex containing ethylenediamine and cyanide as ligands showed 20–30% catalytic activity [17]. These observations highlight the role of the precursor in determining the crystal structure of metal oxides and their catalytic properties. In this work, we present the formation of porous  $\text{Co}_3\text{O}_4$  from  $\text{Co}_3[\text{Co}(\text{CN})_6]_2$  by both thermal decomposition and microwave synthesis and its application towards Li-ion battery.

## 2. Results and discussion

### 2.1. Synthesis and characterization of $\text{Co}_3[\text{Co}(\text{CN})_6]_2$

The precipitate  $\text{Co}_3[\text{Co}(\text{CN})_6]_2 \cdot 12\text{H}_2\text{O}$  was obtained by mixing the solutions of cobalt acetate and potassium hexacyano cobaltate (III). The product can easily be identified by its reversible color transitions in hydrated and dehydrated forms. Similar observations were reported in the literature and attributed to the inter conversion of octahedral to tetrahedral co-ordination of  $\text{Co}^{2+}$  site [18]. The compound was further confirmed by using FT-IR and XRD analysis.

### 2.2. Phase composition analysis

From TGA results (Fig. S1A), it was observed that the

\* Corresponding author.

E-mail address: [jameskavalam@yahoo.com](mailto:jameskavalam@yahoo.com) (J. Joseph).

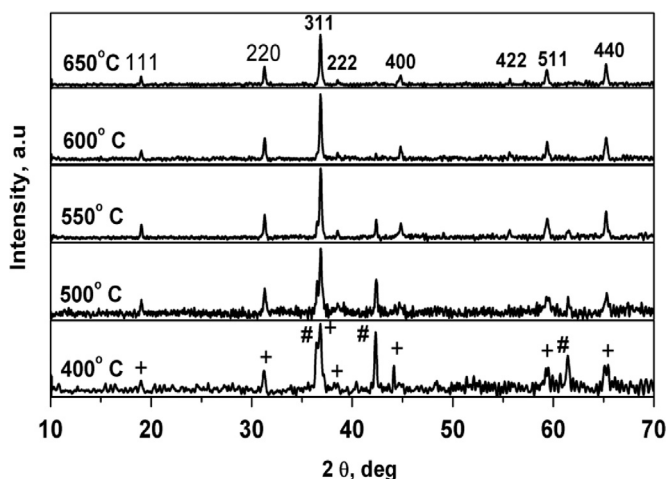


Fig. 1. XRD of cobalt oxide prepared at different temperature. (#) CoO phase and (+)  $\text{Co}_3\text{O}_4$  phase.

decomposition of cyanide ligands is completed below  $350^\circ\text{C}$  and hence we have synthesized cobalt oxides by fixing the temperature at  $400\text{--}650^\circ\text{C}$  in mixed  $\text{Ar}/\text{O}_2$  atmosphere. XRDs were recorded for the samples prepared from decomposition of  $\text{Co}_3[\text{Co}(\text{CN})_6]_2$  at different temperatures (Fig. 1). From the XRD results, it is confirmed that pure  $\text{Co}_3\text{O}_4$  (JCPDS no. 01–078–1969) was formed at  $650^\circ\text{C}$  (decomposition temperature) and this temperature, the calculated crystallite size (using Scherrer equation) value ( $d=8.3\text{ nm}$ ) of  $\text{Co}_3\text{O}_4$  for 311 plane was higher than the value obtained at  $400^\circ\text{C}$  ( $d=2.1\text{ nm}$ ). This implies that the existence of the CoO oxides (JCPDS no: 01–078–0431) phase at a lower temperature may be due to the initial conversion of  $\text{Co}_3[\text{Co}(\text{CN})_6]_2$  partly to cobalt metal and then to metal oxides, viz. CoO and  $\text{Co}_3\text{O}_4$ . This mechanism is suggested because the cyanide ions can act as a reducing agent during thermal decomposition [19]. The two well defined sharp peaks at  $574$  and  $663\text{ cm}^{-1}$  observed [20] in FT-IR spectra (Fig. S1B) were confirmed as due to the  $\text{Co}_3\text{O}_4$  formation.

### 2.3. Morphology and particle distribution

Decomposition of  $\text{Co}_3[\text{Co}(\text{CN})_6]_2$ , results in a significant change in the mass of the sample. The possible decomposition products in the mixed  $\text{Ar}/\text{O}_2$  atmosphere are  $\text{H}_2\text{O}$ ,  $\text{CO}_2$ ,  $(\text{CN})_2$  and  $\text{N}_x\text{O}_y$  [20]. The release of these gaseous products could produce highly porous metal oxide materials and these were confirmed by SEM images of porous  $\text{Co}_3\text{O}_4$  prepared at different temperatures (shown in Fig. 2). We can observe that porous structure in  $\text{Co}_3\text{O}_4$  was retained irrespective of the temperature but the pore size has shown an increase with temperature (Table S1). It is clear from the SEM micrographs that the particle size increases with increasing temperature from  $400$  to  $650^\circ\text{C}$ . This observation is attributed to the aggregation of particles at elevated temperatures. As the temperature increases, the small nanocrystals grow into an interconnected porous structure. Recently, a similar observation is made by Chen et al., during  $\text{Co}_3\text{O}_4$  formation on calcination of  $\text{Co}(\text{OH})_2$  [21]. The shape and particle size of the  $\text{Co}_3\text{O}_4$  was analyzed from TEM studies. Large void spaces present in  $\text{Co}_3\text{O}_4$  can be clearly seen from SEM image shown in Fig. 2A. It is interesting to know that  $\text{Co}_3[\text{Co}(\text{CN})_6]_2$  is active in the microwave region and hence microwave irradiation can also be followed to decompose  $\text{Co}_3[\text{Co}(\text{CN})_6]_2$ . Surprisingly, the microwave assisted synthesis also resulted in the porous cobalt and also existence of cobalt oxide (Fig. 2B) in two different phases c.a.  $\text{Co}_3\text{O}_4$  and CoO. Phase pure  $\text{Co}_3\text{O}_4$  can also be synthesized by optimizing the microwave power and irradiation time. However, more studies are needed to optimize the formation of phase pure  $\text{Co}_3\text{O}_4$  by microwave heating.

### 2.4. Electrochemical studies against $\text{Li}^+/\text{Li}^0$

We have also examined the electrochemical behavior of the pure  $\text{Co}_3\text{O}_4$  as an anode material for Lithium ion battery. Fig. 3A shows the plot of specific capacity ( $\text{mA h g}^{-1}$ ) vs voltage ( $\text{V vs Li}^+/\text{Li}^0$ ) obtained for the charge–discharge profiles of the first, fifth and tenth cycles. Fabricated coin cells were cycled at a rate of  $C/2$  from  $3.0\text{ V}$  to  $0\text{ V}$ . Fig. 3B shows discharge capacity versus cycle number for porous  $\text{Co}_3\text{O}_4$  at  $C/2$  rate. The discharge capacity of the first cycle was found to be as high as  $1131\text{ mA h g}^{-1}$

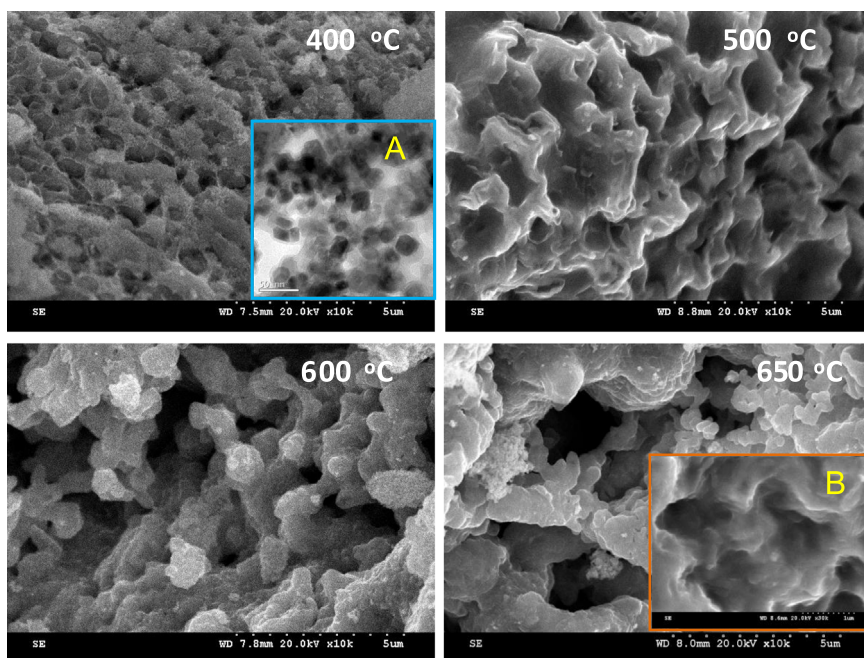
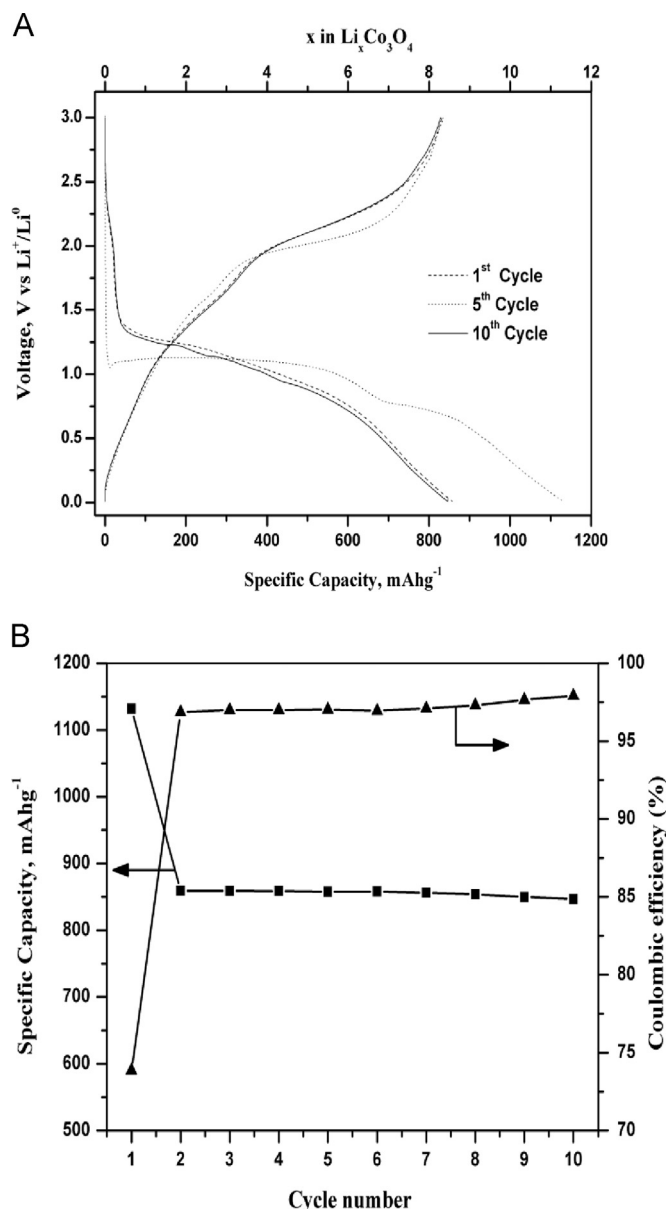


Fig. 2. SEM image of cobalt oxide prepared at different temperatures. Inset figure (A) is TEM image of  $\text{Co}_3\text{O}_4$  obtained at  $650^\circ\text{C}$  and (B) SEM image of  $\text{Co}_3\text{O}_4$  obtained from microwave synthesis.



**Fig. 3.** (A) First, Fifth, Tenth discharge and charge cycle of porous  $\text{Co}_3\text{O}_4$  at  $C/2$  rate. (B) Discharge capacity versus cycle number for porous  $\text{Co}_3\text{O}_4$  at  $C/2$  rate.

(corresponding to  $x=11.3$ ). These are generally attributed to the conversion of  $\text{Co}_3\text{O}_4$  to an intermediate-phase  $\text{CoO}$  (or  $\text{Li}_x\text{Co}_3\text{O}_4$ ) and then to metallic Cobalt, respectively [1,7]. The sloping region may be due to the formation of a solid electrolyte interface (SEI) which leads to an irreversible capacity loss [4]. On charging, a distinct plateau was seen at 1.95 V which corresponds to the formation of a less lithiated phase ( $\text{Li}_n\text{Co}_3\text{O}_4$ ,  $n < x$ ) with a delivering capacity of  $838 \text{ mA h g}^{-1}$  (corresponding to  $x=8.4$ ) and 74% coulombic efficiency. Irreversible capacity loss experienced in the first cycle is due to the incomplete decomposition of  $\text{Li}_2\text{O}$  and SEI formation which is not followed in subsequent cycles [9].

### 3. Conclusions

Here, we have shown a facile route for the synthesis of porous  $\text{Co}_3\text{O}_4$  from prussian blue analog,  $\text{Co}_3[\text{Co}(\text{CN})_6]_2$ . This method for the preparation of nanostructured phase pure metal oxide with high porosity is simple. The formation of the pure  $\text{Co}_3\text{O}_4$  phase

was optimized by varying the temperature between  $400^\circ\text{C}$  and  $650^\circ\text{C}$ . During the thermal decomposition of  $\text{Co}_3[\text{Co}(\text{CN})_6]_2$ , a large change in mass and expulsion of gases take place resulting in the formation of a porous cobalt oxide as evident from SEM and TEM images.  $\text{Co}_3\text{O}_4$  is a promising anode material in Li-ion battery. This porous nano-structured material may help to increase the battery performance by adjusting volume variation occurring during the charge–discharge process. Further possibility of the synthesis of mixed metal hexacyanocobaltates with two or three metal ions  $\text{Ni}^{2+}$  or  $\text{Mn}^{2+}$  with hexacyanocobaltate ions are expected to lead to the synthesis of newer mixed oxides which may have promising application as advanced energy materials and is in progress.

### Acknowledgments

This work was supported by the Department of Science & Technology, New Delhi, India through a Grant-in-aid programme [SR/S1/PC-22/2007]. S. Harish and A.V. Narendrakumar thank CSIR (India) for the award of Senior Research Fellowships.

### Appendix A. Supplementary material

Supplementary data associated with this article can be found in the online version at <http://dx.doi.org/10.1016/j.matlet.2015.11.122>

### References

- [1] P. Poizot, S. Laruelle, S. Grugeon, L. Dupont, J.M. Tarascon, Nano-sized transition-metal oxides as negative-electrode materials for lithium-ion batteries, *Nature* 407 (2000) 496–499, <http://dx.doi.org/10.1038/35035045>.
- [2] L. Hou, C. Yuan, L. Yang, L. Shen, F. Zhang, X. Zhang, Urchin-like  $\text{Co}_3\text{O}_4$  microspherical hierarchical superstructures constructed by one-dimension nanowires toward electrochemical capacitors, *RSC Adv.* 1 (2011) 1521, <http://dx.doi.org/10.1039/c1ra00312g>.
- [3] W.Y. Li, L.N. Xu, J. Chen,  $\text{Co}_3\text{O}_4$  nanomaterials in lithium-ion batteries and gas sensors, *Adv. Funct. Mater.* 15 (2005) 851–857, <http://dx.doi.org/10.1002/adfm.200400429>.
- [4] M. Casas-Cabanas, G. Binotto, D. Larcher, A. Lecup, V. Giordani, J.-M. Tarascon, Defect chemistry and catalytic activity of nanosized  $\text{Co}_3\text{O}_4$ , *Chem. Mater.* 21 (2009) 1939–1947, <http://dx.doi.org/10.1021/cm900328g>.
- [5] T. Sugimoto, E. Matijević, Colloidal cobalt hydrous oxides. Preparation and properties of monodispersed  $\text{Co}_3\text{O}_4$ , *J. Inorg. Nucl. Chem.* 41 (1979) 165–172, [http://dx.doi.org/10.1016/0022-1902\(79\)80506-0](http://dx.doi.org/10.1016/0022-1902(79)80506-0).
- [6] D. Larcher, G. Sudant, J.-B. Leriche, Y. Chabre, J.-M. Tarascon, The electrochemical reduction of  $\text{Co}_3\text{O}_4$  in a Lithium cell, *J. Electrochem. Soc.* 149 (2002) A234, <http://dx.doi.org/10.1149/1.1435358>.
- [7] S. Xiong, J.S. Chen, X.W. Lou, H.C. Zeng, Mesoporous  $\text{Co}_3\text{O}_4$  and  $\text{CoO}@C$  topotactically transformed from chrysanthemum-like  $\text{Co}(\text{CO}_3) \cdot 0.11\text{H}_2\text{O}$  and their lithium-storage properties, *Adv. Funct. Mater.* 22 (2012) 861–871, <http://dx.doi.org/10.1002/adfm.201102192>.
- [8] M.M. Rahman, J.-Z. Wang, X.-L. Deng, Y. Li, H.-K. Liu, Hydrothermal synthesis of nanostructured  $\text{Co}_3\text{O}_4$  materials under pulsed magnetic field and with an aging technique, and their electrochemical performance as anode for lithium-ion battery, *Electrochim. Acta* 55 (2009) 504–510, <http://dx.doi.org/10.1016/j.electacta.2009.08.068>.
- [9] X. Huang, X. Zhao, Z. Wang, L. Wang, X. Zhang, Facile and controllable one-pot synthesis of an ordered nanostructure of  $\text{Co}(\text{OH})_2$  nanosheets and their modification by oxidation for high-performance lithium-ion batteries, *J. Mater. Chem.* 22 (2012) 3764, <http://dx.doi.org/10.1039/c2jm16109e>.
- [10] M.B. Zakaria, M. Hu, R.R. Salunkhe, M. Pramanik, K. Takai, V. Malgras, et al., Controlled Synthesis of nanoporous nickel oxide with two-dimensional shapes through thermal decomposition of metal-cyanide hybrid coordination polymers, *Chem.: A Eur. J.* 21 (2015) 3605–3612, <http://dx.doi.org/10.1002/chem.201404895>.
- [11] M.B. Zakaria, M. Hu, M. Imura, R.R. Salunkhe, N. Umezawa, H. Hamoudi, et al., Single-crystal-like nanoporous spinel oxides: a strategy for synthesis of nanoporous metal oxides utilizing metal-cyanide hybrid coordination polymers, *Chem.: A Eur. J.* 20 (2014) 17375–17384, <http://dx.doi.org/10.1002/chem.201404054>.
- [12] Y. Wang, H.J. Zhang, J. Wei, C.C. Wong, J. Lin, A. Borgna, Crystal-match guided formation of single-crystal tricobalt tetraoxygen nanomesh as superior anode for electrochemical energy storage, *Energy Environ. Sci.* 4 (2011) 1845, <http://dx.doi.org/10.1039/c1ee01845a>.

- [//dx.doi.org/10.1039/c0ee00802h](http://dx.doi.org/10.1039/c0ee00802h).
- [13] J. Ma, A. Manthiram, Precursor-directed formation of hollow  $\text{Co}_3\text{O}_4$  nanospheres exhibiting superior lithium storage properties, *RSC Adv.* 2 (2012) 3187, <http://dx.doi.org/10.1039/c2ra20092a>.
- [14] N. Du, H. Zhang, B.D. Chen, J.B. Wu, X.Y. Ma, Z.H. Liu, et al., Porous  $\text{Co}_3\text{O}_4$  nanotubes derived from  $\text{Co}_4(\text{CO})_{12}$  clusters on carbon nanotube templates: a highly efficient material for Li-battery applications, *Adv. Mater.* 19 (2007) 4505–4509, <http://dx.doi.org/10.1002/adma.200602513>.
- [15] M. Hu, A.A. Belik, M. Imura, K. Mibu, Y. Tsujimoto, Y. Yamauchi, Synthesis of superparamagnetic nanoporous iron oxide particles with hollow interiors by using prussian blue coordination polymers, *Chem. Mater.* 24 (2012) 2698–2707, <http://dx.doi.org/10.1021/cm300615s>.
- [16] R. Weiss, Y. Guo, S. Vukojević, L. Khodeir, R. Boese, F. Schüth, et al., Catalytic activity of copper oxide/zinc oxide composites prepared by thermolysis of crystallographically defined bimetallic coordination compounds, *Eur. J. Inorg. Chem.* (2006) 1796–1802, <http://dx.doi.org/10.1002/ejic.200600005> 2006.
- [17] R. Weiss, S. Vukojević, C. Baltès, R.N. d'Alnoncourt, M. Muhler, M. Epple, Copper/Zinc-tartrates: mixed crystals and thermolysis to a mixture of copper oxide and zinc oxide that is catalytically active in methanol synthesis, *Eur. J. Inorg. Chem.* (2006) 4782–4786, <http://dx.doi.org/10.1002/ejic.200600561> 2006.
- [18] G.W. Beall, D.F. Mullica, W.O. Milligan, Reinterpretation of the structural and physical property changes in the dehydration of  $\text{Co}_3[\text{Co}(\text{CN})_6]_2 \cdot 12\text{H}_2\text{O}$ , *Inorg. Chem.* 19 (1980) 2876–2878, <http://dx.doi.org/10.1021/ic50212a004>.
- [19] M. Vondrova, T.M. McQueen, C.M. Burgess, D.M. Ho, A.B. Bocarsly, Auto-reduction of Pd–Co and Pt–Co cyanogels: exploration of cyanometalate coordination chemistry at elevated temperatures, *J. Am. Chem. Soc.* 130 (2008) 5563–5572, <http://dx.doi.org/10.1021/ja8009764>.
- [20] M. Heibel, G. Kumar, C. Wyse, P. Bukovec, A.B. Bocarsly, Use of sol–gel chemistry for the preparation of cyanogels as ceramic and alloy precursors, *Chem. Mater.* 8 (1996) 1504–1511, <http://dx.doi.org/10.1021/cm960105u>.
- [21] X. Chen, J.P. Cheng, Q.L. Shou, F. Liu, X.B. Zhang, Effect of calcination temperature on the porous structure of cobalt oxide micro-flowers, *CrystrEngComm* 14 (2012) 1271, <http://dx.doi.org/10.1039/c1ce05943b>.